Organic & Biomolecular Chemistry

ARTICLE

A Theoretical Investigation of Substituent Effects on the Stability and Reactivity of *N*-Heterocyclic Olefin Carboxylates

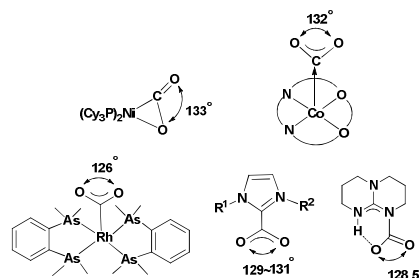Liang Dong,[a] Jun Wen[*a] and Weiyi Li[*b]

A theoretical study of substituent effects on the stability and reactivity of novel synthesized *N*-heterocyclic olefin (NHO) carboxylates has been performed using a combination of density functional theory (DFT) calculations, molecular electrostatic potential (MESP) minimum and nucleophilicity indices analyses. These calculations demonstrate that the nucleophilicity of free NHO is stronger than that of the NHO−CO_2 adduct and, hence, the thermally unstable NHO−CO_2 adduct should be a more efficient organocatalyst for nucleophile-mediated reactions. The stability of the NHO−CO_2 adduct, as well as the reactivity of free NHO, is strongly dependent on the electronic and steric effects of the C- and N-substituents on the imidazole ring. This dependency is reflected by the measured MESP minimum for the carboxylate moiety, NHO−CO_2 adduct (V_{min1}), and the terminal carbon atom of free NHO (V_{min2}). C-substituents exert only electronic effects while N-substituents exert both electronic and steric effects. In general, the electron-withdrawing groups on the C- and N-positions favor decarboxylation while weakening the reactivity of NHO. These positions favor decarboxylation due to the simultaneous decrease of the electronic density on the carboxyl moiety of the NHO−CO_2 and the terminal carbon atom of olefins. Additionally, the balance between the stability of the NHO−CO_2 and the reactivity of free NHO can be tuned by the combined effects of the C- and N-substituents. The introduction of weak electron-withdrawing groups at the C-position and aromatic substituents or similar ring-strained entities at the N-position favors decarboxylation of the NHO−CO_2 adduct and ensures the free NHO as a strong nucleophile.

Introduction

In recent decades, the sequestration, activation, and catalytic transformation of carbon dioxide (CO_2) have attracted much attention because of the steadily increasing concentration of CO_2 in the atmosphere and the advantages of being a non-toxic, renewable, abundant, and economical C1 source.[1] However, relative to other common C1 sources (e.g. carbon monoxide and phosgene), CO_2 is thermodynamically stable and kinetically inert since it exists in the highest possible oxidation state. Highly active reagents (e.g. Grignard reagents and small-membered ring compounds), powerful catalysts, high reaction temperatures, and high pressure are usually required for the successful incorporation of CO_2 into value-added chemicals.[2] Consequently, much effort has been devoted to the development of more effective catalytic systems for CO_2 activation.

Based on the difference in electronegativity between carbon and oxygen atoms, CO_2 acts as an electrophile. Thus, low-valence metal reagents and strong nucleophiles are often chosen to activate CO_2. Nucleophilic nickel(0),[3a,b] cobalt(I),[3c] and Rh(I)[3d] have been successfully used to bond CO_2 as a η^1 or η^2 ligand (Scheme 1). In these CO_2-based complexes, the activation of CO_2 is indicated by the bent geometry of the binding CO_2 moiety. This moiety has an O−C−O angle in the range of 126º-133º, which is different from the nonpolar linear structure of free CO_2. On the other hand, metal-free nucleophiles for CO_2 activation based on carbon, nitrogen, and oxygen have been demonstrated as well. In particular, *N*-heterocyclic carbenes (NHCs)[2a,4], with a lone pair of electrons on the carbene atom, have received considerable attention as nucleophiles because they show good affinity for CO_2. This reaction generates imidazolium carboxylates, which are the adducts of NHCs and CO_2. Lu[5a] and Louie[5b] synthesized and characterized a series of *N*,*N*'-di-substituted NHC−CO_2 adducts.

[a] *Institute of Nuclear Physics and Chemistry, China Academy of Engineering Physics, 621900, Mianyang, Sichuan, P. R. China.*
[b] *School of Science, Xihua University,610039, Chengdu, Sichuan, P. R. China.*
† E-mail address: weiyili@mail.xhu.edu.cn (W. Li), junwen@caep.cn (J. Wen); Tel: +86-028-87727663; Fax: +86-028-87727663;
Electronic Supplementary Information (ESI) available: Computational details, optimized geometries, calculated energies and the full citation of Gaussian 09 program. See DOI: 10.1039/x0xx00000x

Scheme 1 Typical CO_2-based complexes.

The bent geometry of the CO_2 moiety with an O−C−O angle of 126º-133º was reported for these NHC−CO_2 adducts. This geometry was confirmed using single-crystal X-ray analysis, providing evidence for the activation of CO_2 by the lone pair of carbene electrons. Investigations of the thermal stability of these adducts using *in situ* FTIR and thermogravimetric analysis (TGA) indicated that, as steric bulk on the N-substituent increased, the decarboxylation of NHC−CO_2 adducts became easier.[5b] Subsequently, Suresh and co-workers carried out a DFT study on the assessment of electronic and steric properties of *N*- and *C*-substituents. This work demonstrated the impact of *N*- and *C*-substituents on the CO_2 fixation ability of NHCs in terms of molecular electrostatic potential (MESP) analysis.[5c] Their theoretical results revealed that the N-substituents predominantly contributed steric effects on the carbene center while the C-substituents exerted electronic effects. Placement of electron-donating groups at the C-position and less sterically hindered groups at the N-position favors an increase of the electronic-rich character of the carbene center and the fixation ability for CO_2. In addition, NHC−CO_2 adducts also have been used as organocatalysts to promote the chemical transformation of CO_2 into a number of useful organic compounds such as methane, methanol, carboxylic acid, cyclic carbonates, oxazolidones, and their derivatives.[6] However, in most catalytic systems, the catalytic role of the NHC−CO_2 adduct is unclear. It is hard to determine whether the catalytically active species is free NHC or the NHC−CO_2 adduct because the NHC-CO_2 adduct and free NHC exist in equilibrium. Various theoretical studies on the mechanisms of these reactions indicate that free NHCs serve as catalyst precursors or actual catalytic species due to their high nucleophilicity.[7]

The aromatization of the *N*-heterocyclic ring in *N,N'*-disubstituted-2-methylene imidazolines makes the terminal carbon atom electronegative. These *N*-heterocyclic olefins (NHO), similar to NHCs, are also potential nucleophiles for the capture, activation, and transformation of CO_2.[8] More recently, Lu and co-workers[9] reported the first example of the synthesis of a series of *N,N'*-disubstituted NHO−CO_2 adducts using 2-methyl imidazolium iodide as a starting material (Scheme 2). Meanwhile, the geometries, thermal stabilities, and catalytic activities of these NHO-CO_2 adducts were investigated and compared with the corresponding NHC−CO_2 adducts. The experimental results suggested that, in an organic solvent, a dynamic equilibrium exists between the NHO−CO_2 adduct, free CO_2 and the corresponding NHO. Both the NHO−CO_2 adduct and the NHO produced might serve as a nucleophilic catalyst to promote the carboxylative cyclization of CO_2 and propargylic alcohols into α-alkylidene cyclic carbonates. It was also observed that the alkyl substituents on the N-position of the imidazolium compound influenced the decarboxylation rate of NHO−CO_2 adducts and their catalytic activities. These results are compatible with previous experimental and theoretical results that showed the CO_2 fixation ability of NHCs was closely related to the stereoelectronic effect of N- and C-substituents, and ring fusion on the imidazolium ring.[5] Inspired by these findings, we hypothesized that the electronic and steric effects of N- and C-substituents might also affect the stability and catalytic activity of various NHO−CO_2 organocatalysts. In the present work, we carry out a systematic theoretical investigation to assess the factors that influence the electronic and steric effects on NHO−CO_2 organocatalysts. We aim to provide useful information for designing more efficient NHO catalysts with the desired electronic and steric demands by modeling the decarboxylation of NHO−CO_2 adducts in a solvent.
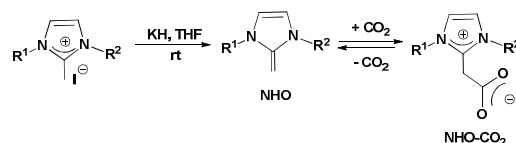
Scheme 2 The synthesis of NHO and NHO−CO_2 adducts.

Computational Details

All calculations were performed using DFT within the Gaussian 09 software package.[10] The M06-2X functional,[11] plus the continuum solvation model (SMD[12]) with the standard 6-31++G(d,p) basis set,[13] were used to optimize the structures of the reactants, products, intermediates, and transition states in CH_2Cl_2 solvent (experimentally used) at 298.15 K. The solute cavity was redefined with radii=UAHF, because this atomic cavity was found to be more suitable than the default atom cavity (radii=SMD-Coulomb) defined in the SMD model (Table 1 and S1-S4 in ESI). The vibrational frequencies were calculated using the same level to characterize each optimized-structure as an intermediate (no imaginary frequency) or a transition state (unique imaginary frequency), and then obtain the thermal corrections at 298.15 K. The energies were then improved by single-point energies in CH_2Cl_2 solvent at the M06-2X/6-311++(2d,2p) level, and correction of the basis set superposition errors (BSSE[14]). Since the present calculations were performed in liquid phase, a concentration correction of 1.89 kcal mol^{-1} was applied for the free energy (G_{sol}) to account for the change from a standard state of 1 atm to a standard state of 1 mol L^{-1}.[15] The final free energies for all the species were summarized in Table S5-S8 in ESI.

Furthermore, the wave function generated at the [SMD, M06-2X/6-31++G(d,p)] level was used for MESP analysis,[16] which has been widely and successfully used as an efficient electronic descriptor to quantify the substituent effect in NHC[5c] analogs and other organic systems.[17] The MESP at the carboxylate groups in NHO−CO_2 adducts (V_{min1}) and terminal carbon atoms on free NHOs (V_{min2}) were measured by the Multiwfn program.[18] The global nucleophilicity indices[19] of the NHO−CO_2 adducts (N_1) and free NHOs (N_2), defined as $N = E_{HOMO(Nu)} - E_{HOMO(TCE)}$,[20] were calculated based on the HOMO energies of the ground states of the molecules obtained at the M06-2X/6-311++G(2d,2p) level. The graphics of three-dimensional molecular structures and the visualization of the MESP for molecular structures were drawn using CYLVIEW[21] and the VMD program,[22] respectively.

2 | *Org. Biomol. Chem.*, 2015, **00**, 1-3

This journal is © The Royal Society of Chemistry 20xx

Organic & Biomolecular Chemistry　　　　　　　　　　　　　　　　　　**ARTICLE**

Results and Discussion

Commentary on the computational protocol

First, geometric optimization and frequency calculations for a series of NHO–CO$_2$ adducts (**2a**-**2g**) reported by Lu and co-workers[9] were carried out in the gas phase using B3LYP and M06-2X with the 6-31++G(d,p) basis set. Calculations in CH$_2$Cl$_2$ were then performed using SMD model. This model and calculation were done to determine the appropriate computational method for our system. Figure 1 displays the optimized structures of the NHO–CO$_2$ adducts (**2a**-**2g**). Geometrical parameters and the IR frequency of the carboxylate C=O stretching in the NHO–CO$_2$ adduct **2g** obtained from the above computational methods and the corresponding experimental data are summarized in Table 1. The computed results for the other NHO–CO$_2$ adducts are available in the ESI.
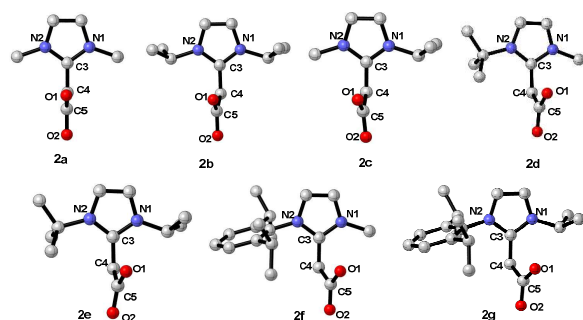

Figure 1 Optimized structures of NHO–CO$_2$ adducts.

Table 1 Comparison of experimental data with the computed results for the NHO–CO$_2$ adduct 2g.

| Parameters	B3LYP Gas Phase	B3LYP CH$_2$Cl$_2$	M06-2X Gas Phase	M06-2X CH$_2$Cl$_2$ ^{a}	M06-2X CH$_2$Cl$_2$ ^{b}	EXP data[9]
C3–C4 (Å)	1.465	1.483	1.468	1.480	1.479	1.476
C4–C5 (Å)	1.643	1.565	1.621	1.557	1.584	1.568
N1–C3–N2(°)	106.9	107.2	107.1	107.2	107.2	106.7
O1–C5–O2(°)	133.5	127.3	133.1	129.5	127.2	129.1
N1–C3–C4–C5(°)	74.3	74.5	72.6	69.7	70.2	74.9
N2–C3–C4–C5(°)	98.4	105.8	99.3	105.6	108.1	106.5
C3–C4–C5–O1(°)	27.9	5.3	19.5	6.0	10.7	7.9
C3–C4–C5–O2(°)	153.0	175.5	160.9	174.9	170.4	172.7
C=O stretching frequency (cm^{-1})	1778	1620	1826	1674	1732	1645

a: The atom cavity defined with radii=UAHF; *b*: The atom cavity defined with radii= SMD-Coulomb.

The geometric parameters for the NHO–CO$_2$ adducts optimized by both B3LYP and M06-2X methods in the gas phase deviated somewhat from the data of the single-crystal structure of the corresponding NHO-CO$_2$ adducts. For example, the C4–C5 bond lengths, the C1–O5–C2 bond angles, and the C3–C4–C5–O1 dihedral angles in the gas-phase for sample **2g** are significantly greater than determined from the single

crystal structure (Table 1). The computed IR frequency for C=O stretching of the carboxylate group in a vacuum (1778 and 1826 cm^{-1}) is at a much higher than observed in the experiment (1645 cm^{-1}).[9] In contrast, both geometries of the NHO–CO$_2$ adducts in CH$_2$Cl$_2$ correspond well to the single-crystal structure. Differences between bond lengths were less than 0.01 Å, between bond angles and dihedral angles were less than 5.0° from both the B3LYP and the M06-2X method. The calculated frequencies of the C=O stretching of the carboxylate moiety (1620 and 1674 cm^{-1}) were also close to the corresponding experimental data.[9] These results indicate that the solvent may have a greater impact on the molecular geometries of the NHO–CO$_2$ adducts than we anticipated. In addition, the atomic cavity defined with radii=UAHF was found to be more suitable than the default atomic cavity in SMD model. With respect to Becke's three-parameter exchange functional (B3LYP), the hybrid *meta* exchange-correlation functional (M06-2X) has been proved to perform well in thermochemistry, kinetics, and non-covalent interactions.[11] For our work, we believe that the M06-2X functional will give more accurate energetic calculations than the B3LYP functional. Thus, the geometric optimization and energetic calculations for all the species involved in the present system were carried out at the M06-2X(SMD, CH$_2$Cl$_2$)/6-311++G(d,p) level, together with radii=UAHF.

Substituent effects on the stability and reactivity of NHO–CO$_2$ adducts

To investigate the substituent effects on the stability and reactivity of the NHO–CO$_2$ adducts and free NHOs, four sets of NHO–CO$_2$ adducts and the corresponding NHOs, bearing different kinds of substituents on the carbon or nitrogen atom of the imidazolium ring, were studied in the present work. As shown in Scheme 3, set A includes NHO–CO$_2$ adducts with the same substituents (R^3) on the carbon atoms, and set B includes NHO–CO$_2$ adducts with symmetrical or dis-symmetrical substituents (R^1 and R^2) on the nitrogen atoms. Set C includes substituents on both carbon and nitrogen atoms of the imidazolium ring and set D consisted of some miscellaneous NHO–CO$_2$ adducts with ring fusions on the carbon and nitrogen atoms simultaneously. Decarboxylation of NHO–CO$_2$ was simulated in CH$_2$Cl$_2$ for each of the four sets so that an assessment of the stability of the NHO–CO$_2$ adduct could be made. The calculations indicate that the decomposition of NHO–CO$_2$ proceeds through a transition state with the cleavage of the C4–C5 bond (Figure2), leading to the generation of free NHOs and CO$_2$. The activation free energy barrier ($\Delta G^{\neq}$) can be used to assess the kinetic stability of the NHO–CO$_2$ adducts. The thermal stability of the NHO–CO$_2$ adducts can be evaluated by the reaction free energy (ΔG_{rxn}), which is defined as the difference between the free energy of the NHO–CO$_2$ adduct and the sum of the free energies of its subsystems (NHO and CO$_2$).
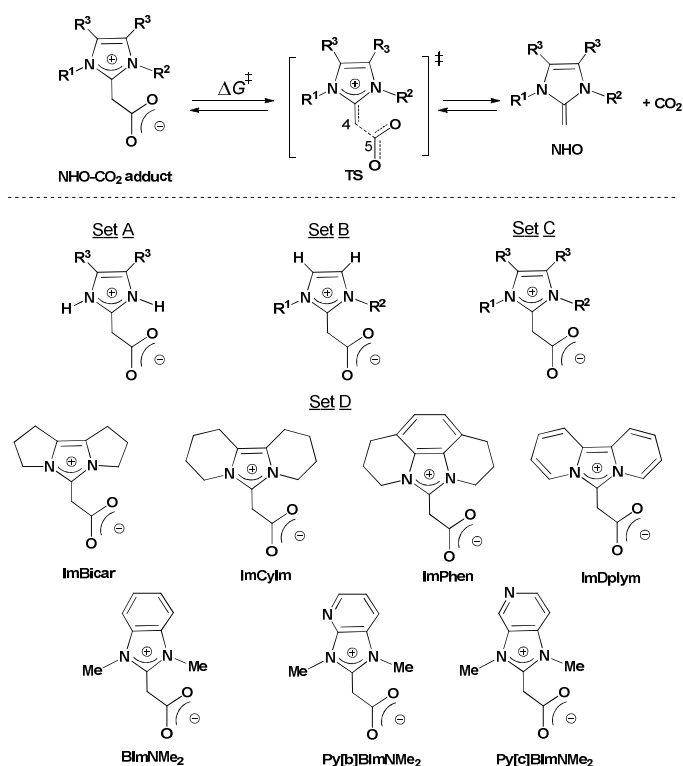
Scheme 3 Simulation of decarboxylation of selected NHO−CO$_2$ adducts with different substituents on the carbon and nitrogen atoms of the imidazolium ring.
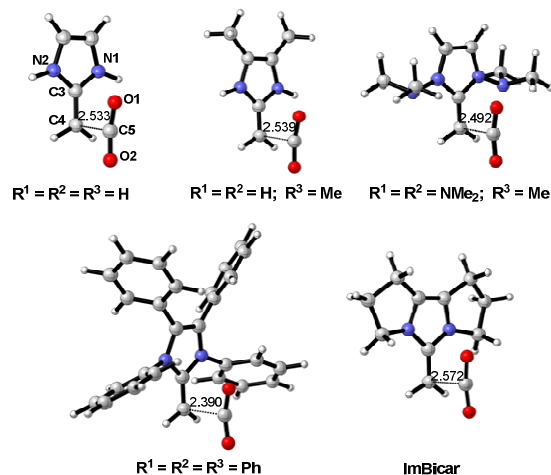

Figure 2 Optimized-structures for some representative decarboxylation transition states at the M06-2X/6-31++G(d,p) level (bond lengths are labeled in Å).

Effect of the C-substituents

Various substituents introduced at the C-position (R^3) of the imidazolium ring while the N-positions (R^1 and R^2) are saturated by hydrogen atoms (set A) were studied to explore the effects of the C-substituents on the stability and reactivity of NHO-CO$_2$ adducts. The unsubstituted NHO−CO$_2$ adduct (all N- and C-substituents are hydrogen atoms) was chosen as the reference system. For the NHO−CO$_2$ adducts in set A, an intramolecular hydrogen bond is formed between the H atom on the N-position and one O atom of the carboxylate moiety in

each NHO−CO$_2$ adduct (Figure 3). This hydrogen-bonding interaction leads to a twisted conformation in the structure of NHO−CO$_2$. The degree of distortion was assessed by estimating the values of the two dihedral angles ϑ_1 and ϑ_2 defined in Figure 2 and summarized in Table 2. The MESP analysis on the NHO−CO$_2$ adducts shows that the charge is strongly separated in these moieties while the positive charge is delocalized on the imidazolium ring. A negative MESP minimum (V_{min1}) in the NHO−CO$_2$ adducts always appears at the carboxyl oxygen lone pair region. The charge distribution is similar to that observed

4 | *Org. Biomol. Chem.*, 2015, **00**, 1-3

This journal is © The Royal Society of Chemistry 20xx

in the NHC–CO2 adduct.[5c] For the NHO–CO$_2$ adducts, the relative value of V_{min1} with respect to the reference system (ΔV_{min1}) is used to measure the electronic effect of the C-substituents on the carboxyl group (Table 2). For example, V_{min1} values of –99.0, –97.1, and –83.1 kcal mol^{-1} calculated for the NHC–CO$_2$ adducts with -NMe$_2$ -Ph, and -NO$_2$ groups, respectively, mean that the electronic effect of these groups at the C-position on the carboxyl group are 10.7, 8.8, and –5.2 kcal mol^{-1}, respectively. For the free NHOs, the charge distribution is dependent on the type of substituent that is located at the C-position. The V_{min2} is denoted as a negative-valued MESP around the terminal carbon (C4) of the olefin, although the minimum is not located at this position for some free NHOs containing strong electro-withdrawing groups, such as -CO$_2$Me, -CN, and -NO$_2$ (Figure 3). Similarly, the difference (ΔV_{min2}) between V_{min2} of the NHO and V_{min2} of the reference can give the electronic effect of C-substituents on NHO. The values of V_{min1} and V_{min2} follow the same relative order and show a linear relationship, suggesting that the C-substituents exhibit the same electronic effect in both NHO–CO$_2$ and free NHO. The values of the reaction free energies (ΔG_{rxn}) for the decarboxylation process are all positive (Table 2) for the NHO–CO$_2$ adducts in set A, meaning that the NHO–CO$_2$ adducts are thermodynamically stable in CH$_2$Cl$_2$ at 298 K. When the values of V_{min1} and V_{min2} are less negative, less reaction free energy (ΔG_{rxn}) is required during the decarboxylation process, which means that the NHO–CO$_2$ adducts are more thermodynamically unstable. The order of the corresponding values for the free energy barrier ($\Delta G^{\neq}$)

follows the same trend. Less negative values for V_{min1} and V_{min2} are obtained, indicating that a smaller free energy barrier ($\Delta G^{\neq}$) must be overcome for the decomposition of the NHO–CO$_2$ adducts to occur. Hence, the decomposition of NHO–CO$_2$ would be faster. The NHO–CO$_2$ adducts with electron-donating C-substituents always have high values for both ΔG_{rxn} and $\Delta G^{\neq}$. The highest values for ΔG_{rxn} (22.7 and 22.4 kcal mol^{-1}) and $\Delta G^{\neq}$ (28.4 and 28.7 kcal mol^{-1}) are obtained for the NHO–CO$_2$ adducts with -Me and -NMe$_2$ groups, respectively. In contrast, CO$_2$ is weakly bonded to the NHOs when the C-substituent is an electron-withdrawing group. These calculations predict that NHO–CO$_2$ in combination with a -NO$_2$ group on the C-position has the lowest ΔG_{rxn} (4.6 kcal mol^{-1}), and $\Delta G^{\neq}$ (8.4 kcal mol^{-1}) for decarboxylation. The relationship between the MESP minimum (V_{min1} and V_{min2}) and the MESP minimum (V_{min1} and V_{min2}) and the free energies (ΔG_{rxn} and $\Delta G^{\neq}$) for decarboxylation are plotted in Figure 4. A good linear correlation exists between the MESP minimum and ΔG_{rxn}. The correlation coefficients are 0.93 and 0.92 for set A, respectively. However, the linear correlations are poorer between the MESP minimum and $\Delta G^{\neq}$ (correlation coefficients are 0.73 and 0.79). This poorer correlation might be caused by the intramolecular hydrogen bonding. For NHO–CO$_2$ adducts with electron-donating groups, hydrogen bonding is stronger when the electron-withdrawing groups are introduced at the C-position, which is indicated by shorter N–H···H hydrogen-bond distances (see Figure 3). Stronger intramolecular hydrogen bonding enhances the stability of the NHO–CO$_2$ adduct and somewhat disfavors decarboxylation.
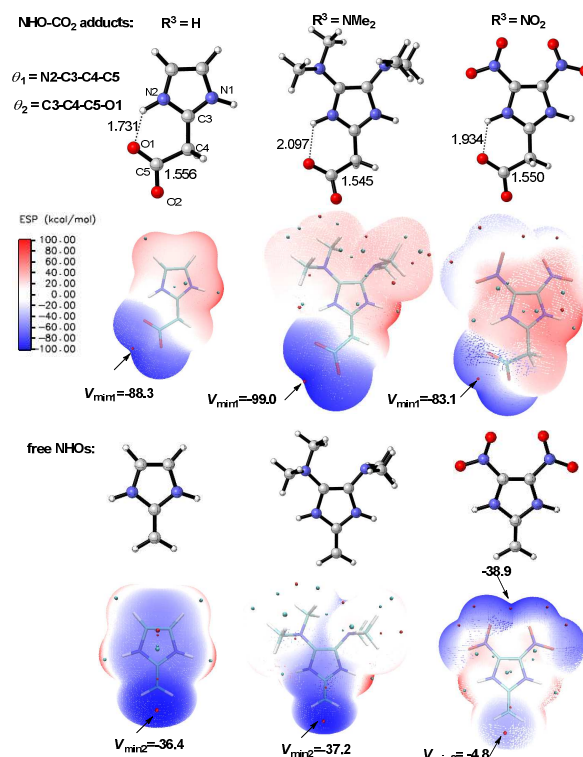

Figure 3 Geometries and the MESP isosurface for some representative NHO–CO$_2$ adducts and free NHOs in set A (bond lengths are labeled in Å, and V_{min} values are given in kcal mol^{-1}).

Table 2 Key bond distance (Å), dihedral angle (º), value of the MESP minimum, activation free energy, reaction free energy (all in kcal mol^{-1}), and nucleophilicity indices (eV) of NHO−CO$_2$ adducts and free NHO in set A.

R^3	d_{C4-C5}	ϑ_1	ϑ_2	$\Delta G^{\neq}$	ΔG_{rxn}	V_{min1}	V_{min2}	N_1	N_2
H	1.489	5.9	8.3	24.9	17.1	−88.3	−36.4	2.0	5.0
Me	1.545	31.3	27.3	28.4	22.7	−99.3	−38.9	2.4	5.1
Me$_2$N	1.545	34.2	33.6	28.7	22.4	−99.0	−37.2	3.1	5.1
MeO	1.544	25.9	27.0	26.0	20.9	−97.1	−34.5	2.7	4.7
Ph	1.558	26.3	29.1	26.5	19.5	−97.1	−32.5	2.9	5.0
F	1.546	28.2	23.4	24.7	15.8	−91.6	−24.2	1.9	4.3
Cl	1.546	28.6	22.9	24.1	15.3	−92.1	−25.5	2.0	4.4
CO$_2$Me	1.548	35.6	27.7	22.2	13.2	−92.5	−26.4	1.8	4.5
CF$_3$	1.548	27.6	24.1	21.1	10.8	−88.1	−18.8	1.6	4.3
CN	1.549	28.4	22.3	18.8	7.2	−84.0	−11.1	1.6	4.2
NO$_2$	1.550	26.6	23.7	8.4	4.6	−83.1	−4.8	1.5	3.9
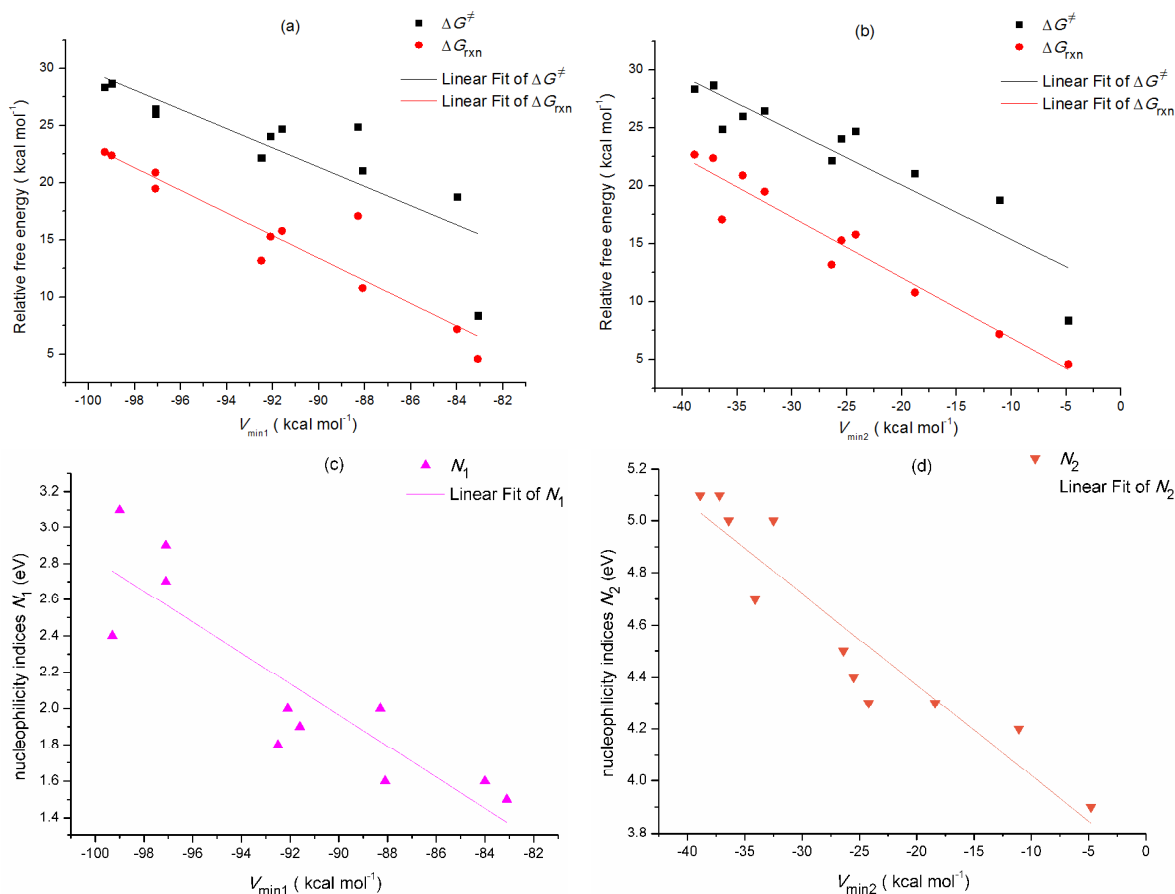
Figure 4 The relationship between the negatively valued MESP minimum (V_{min1} and V_{min2}) and reaction energies ($\Delta G^{\neq}$ and ΔG_{rxn}) for decarboxylation, and nucleophilicity indices (N_1 and N_2) of NHO−CO$_2$ adducts and free NHOs in set A.

The reactivity of the NHO−CO$_2$ adducts and the free NHOs were analyzed using the nucleophilicity index. The nucleophilicity index is used because NHO−CO$_2$ and free NHO usually act as nucleophiles for active CO$_2$. The calculations show that the nucleophilicity index for the free NHO is always larger than for the NHO−CO$_2$ adduct, indicating that the nucleophilicity of free NHO is greater than NHO−CO$_2$. Hence, NHO is classified as strong nucleophiles ($N_2 \geq 3.9$).[23] The unstable NHO−CO$_2$ adduct favors decarboxylation with the generation of highly active catalysts for CO$_2$ transformation.

6 | *Org. Biomol. Chem.*, 2015, **00**, 1-3

This journal is © The Royal Society of Chemistry 20xx

Additionally, we found that the nucleophilicity indices of the NHO–CO_2 adducts and free NHOs correlate to the negatively valued MESP minimums (V_{min1} and V_{min2}) (Figure 4). The more negative the values of V_{min1} and V_{min2}, the larger the values of N_1 and N_2 for NHO–CO_2 adducts and free NHOs, respectively. The free NHOs with electron donating -Me and -NMe_2 groups on the C-position have the strongest nucleophilicity while the nucleophilicity of the free NHOs with -NO_2 group is weakest. As a result, the electronic effect of C-substituents affects the stability of the NHO–CO_2 adducts and the reactivity of free NHOs.

Effect of N-substituents

Hydrogen atoms at the N-position of the imidazolium ring were replaced by different substituents (R^1 and R^2) while the C-positions (R^3) were saturated by hydrogen atoms (set B) for investigation of the effect of N-substituents on the stability of the NHO–CO_2 adducts and the reactivity of free NHOs. The key geometric parameters (d_{C4-C5}, ϑ_1, and ϑ_2), free energies ($\Delta G^{\neq}$ and ΔG_{rxn}) for decarboxylation, values of MESP minima, and nucleophilicity indices (N_1 and N_2) of the NHO–CO_2 adducts and free NHOs in set B are listed in Table 3.

From the point-of-view of the structures of the NHO–CO_2 adducts in set B, the intramolecular hydrogen bonds are broken as substituents are introduced at the N-position. The CO_2 moiety is nearly perpendicular to the plane of NHO with the dihedral angles (ϑ_1) approximately 90° for NHO–CO_2 adducts with symmetrical N-alkyl substituents ($R^1 = R^2 =$ Me, *i*Pr, *t*Bu, Ph, Cy, and 2,6-$^{iPr}C_6H_3$). Except for adducts with bulky 2,6-$^{iPr}C_6H_3$ groups, the two terminal oxygen atoms are nearly coplanar with the C3, C4, and C5 atoms, as indicated by zero or near-zero values of the dihedral angle (ϑ_2). For the adducts with dis-symmetrical N-alkyl substituents, the values of the dihedral angles ϑ_1 are less than 90°, and ϑ_2 has significantly deviated from zero, resulting in a twisted conformation for the CO_2 moiety. These findings are consistent with the single-crystal structures obtained.[9] The larger the sterically encumbering group and dis-symmetric N-alkyl substituents introduced at the N-position, the lower the coplanarity of the CO_2 moiety, and the easier decarboxylation for NHO–CO_2 adduct. Calculations indicate that the decarboxylation of NHO–CO_2 containing a symmetrical bulky 2,6-$^{iPr}C_6H_3$ group has the lowest reaction energies (ca. 15.3 kcal mol^{-1} for ΔG_{rxn} and 23.6 kcal mol^{-1} for $\Delta G^{\neq}$). These calculations agree with experimental observations.[9]

Table 3 Key bond distance (Å), dihedral angle (°), value of the MESP minimum, activation free energy, reaction free energy (all in kcal mol^{-1}), and nucleophilicity indices (eV) of NHO–CO_2 adducts and free NHOs in Set B.

R^1	R^2	d_{C4-C5}	ϑ_1	ϑ_2	$\Delta G^{\neq}$	ΔG_{rxn}	V_{min1}	V_{min2}	N_1	N_2
H	H	1.489	5.9	8.3	24.9	17.1	−88.3	−36.4	2.0	5.0
Me	Me	1.558	87.0	0.0	27.0	20.5	−99.1	−36.2	2.2	5.0
*i*Pr	*i*Pr	1.553	87.0	6.7	33.3	27.5	−99.8	−36.4	2.2	5.1
*t*Bu	*t*Bu	1.558	87.1	6.7	28.2	21.7	−101.2	−35.4	2.3	5.2
Cy	Cy	1.553	88.8	0.1	28.9	22.8	−100.4	−37.5	2.3	5.1
Ph	Ph	1.556	89.6	0.0	25.2	16.7	−97.0	−32.8	2.1	4.8
2,6-$^{iPr}C_6H_3$	2,6-$^{iPr}C_6H_3$	1.559	89.0	19.0	23.6	15.3	−99.5	−32.6	2.2	4.8
Me	*i*Pr	1.557	70.7	1.7	26.4	17.3	−99.4	−36.1	2.2	5.0
Me	*t*Bu	1.558	80.3	9.2	26.4	20.7	−99.7	−35.8	2.2	5.1
*i*Pr	*t*Bu	1.556	80.3	14.0	27.3	21.3	−99.9	−35.8	2.3	5.1
Me	2,6-$^{iPr}C_6H_3$	1.558	66.4	2.6	25.7	11.8	−98.5	−34.2	2.2	4.9
*i*Pr	2,6-$^{iPr}C_6H_3$	1.558	69.7	6.0	26.7	15.0	−98.7	−31.7	2.2	4.9
NMe_2	NMe_2	1.556	84.8	4.0	30.5	23.6	−103.5	−43.3	2.1	4.7
OMe	OMe	1.559	87.3	1.7	24.9	13.8	−91.8	−25.7	2.0	3.9
CF_3	CF_3	1.571	87.3	0.0	11.6	−3.0	−93.8	−19.7	1.8	3.7
CO_2Me	CO_2Me	1.560	42.5	9.5	13.0	−4.2	−91.4	−16.5	1.7	3.7
CN	CN	1.587	68.6	19.5	8.5	−14.0	−87.2	−5.9	1.6	3.6

On the other hand, the electronic effect of N-substituents also influences the stability and reactivity of NHO–CO_2 and NHO in set B. Compared with the reference system ($R^1 = R^2 =$ H), the values of both V_{min1} and V_{min2} for N-alkyl substituted NHO–CO_2 adducts and free NHOs are more negative (Table 3). The stability of NHO–CO_2 increases when the electron-donating group is introduced at the N-position. However, the reaction energies (ΔG_{rxn} and $\Delta G^{\neq}$) for decarboxylation do not linearly

increase with the decrease of V_{min1} and V_{min2}. V_{min1} and V_{min2} for set B significantly deviate from the correlation line obtained for set A (Figure 5). This deviation might be because the steric effect of alkyl substituents has an important effect on the stability of NHO–CO_2. For example, the NHO–CO_2 adduct with -NMe_2 groups possesses the most negatively valued V_{min1} (−103.5 kcal mol^{-1}), but the $\Delta G^{\neq}$ (30.5 kcal mol^{-1}) and ΔG_{rxn} (23.6 kcal mol^{-1}) for decarboxylation are not the

highest. The stability of the NHO–CO_2 adduct is significantly lower with electron-withdrawing groups at the N-position (R^1 = R^2 = -CF_3) relative to NHO–CO_2 with the same substituents at the C-position. This is the case even though both V_{min1} and V_{min2} are more negative for the N-substituted adduct than for the C-substituted adduct (Figure 6). Decarboxylation is

predicted to be thermodynamically spontaneous at room temperature, as suggested by the negative value for ΔG_{rxn} (−3.0 kcal mol^{-1}). The decarboxylation rate is accelerated as the energy barrier ($\Delta G^{\neq}$) is lowered to 11.6 kcal mol^{-1}. This result is attributed to the increase of the steric effect with -CF_3 on the N-positions.

Figure 5 Relationship between the negatively valued MESP minimum (V_{min1} and V_{min2}), and reaction energies ($\Delta G^{\neq}$ and ΔG_{rxn}) for decarboxylation of NHO–CO_2 adducts and free NHOs in set B.
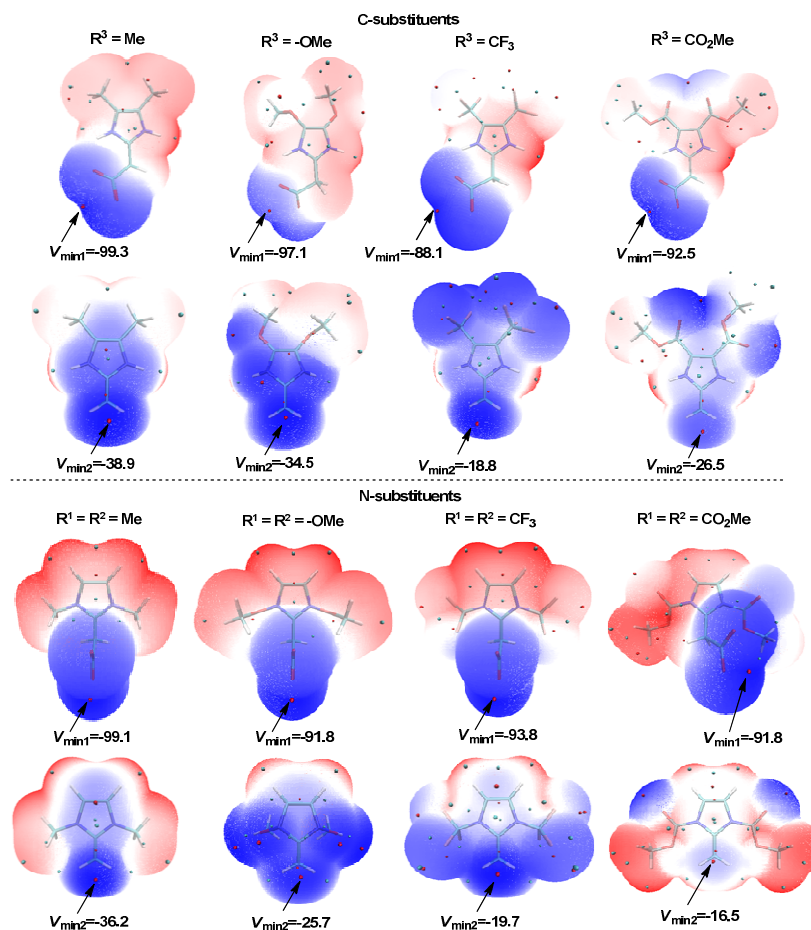
Figure 6 The visualization MESP isosurface of the representative NHO–CO_2 adducts and NHOs in set A and set B (V_{min1} and V_{min2} values are given in kcal mol^{-1}).

8 | *Org. Biomol. Chem.*, 2015, **00**, 1-3

This journal is © The Royal Society of Chemistry 20xx

For NHO–CO$_2$ adducts with -CN and -CO$_2$Me groups as the N-substituents, decarboxylation is predicted to be thermodynamically and kinetically favorable owing to the dramatic decrease in the electronic-rich character of the terminal carbon atom of NHOs. From the analysis in this section, it is clear that the stabilities of NHO–CO$_2$ adducts in set B are dependent on steric as well as electronic effects of N-substituents. This result is different from the result for the NHC system in which the steric effects of N-substituents played the major role in adduct stability.[5] In addition, the nucleophilic reactivity of free NHO is closely related to the electronic effects of the N-substituents (Table 3). Aliphatic groups at the N-position slightly increase the MESP around the terminal carbon atom of NHO, while aromatic groups slightly decrease the nucleophilicity of the NHOs. The electron-donating group, -NMe$_2$, is not as effective at increasing the nucleophilicity of NHO on the N-position relative to the C-positions. This result is similar to the result for the NHC system.[5c] However, when electron-withdrawing groups (R^1 = R^2 = -CO$_2$Me, -CF$_3$, and -CN) are placed at the C-position, the reactivity of free NHOs is significantly decreased, as indicated by the smaller nucleophilicity indices (Table 3). Interestingly, the -OMe group at the N-position serves as an electron withdrawing group and lowers the reactivity of free NHO.

Combined effect of the N- and C-substituents

Since substituent effects are often additive in organic systems, decarboxylation of NHO–CO$_2$ adducts in set C and set D were simulated in order to evaluate the combined effects of both N- and C-substituents on the stability of the NHO–CO$_2$ adduct and reactivity of free NHO. Set C includes NHO–CO$_2$ adducts and free NHOs with normal substituents while set D contains substituents with saturated or unsaturated rings condensed from the imidazole ring.

The MESP of representative NHO–CO$_2$ adducts and the corresponding free NHOs in set C and set D are presented in Figure 7. The geometric parameters (d_{C4-C5}, ϑ_1, and ϑ_2), free energies ($\Delta G^{\neq}$ and ΔG_{rxn}) for decarboxylation, values of minimum MESPs, and nucleophilicity indices (N_1 and N_2) of the NHO–CO$_2$ adducts and free NHOs for set C and set D are summarized in Table 4 and 5, respectively.

Compared with the NHO–CO$_2$ adducts and free NHOs in set A and set B, the electronic effect for the corresponding entities in set C are obviously additive, as shown by the difference of the negatively valued MESP minimums (V_{min1} and V_{min2}). When the electron-donating groups (-Me, -Ph, and -NMe$_2$) are simultaneously introduced at the N- and C-positions of the NHO–CO$_2$ adduct and free NHO, both V_{min1} and V_{min2} are more negative than the ones with only one election-donating group. For the NHO–CO$_2$ adducts and free NHOs bearing election-withdrawing groups (-CO$_2$Me, -CF$_3$, or -CN) at both the N- and C-positions, the additive electronic effect is stronger. This trend is especially true when the value of V_{min2} is positive and four -CN groups are substituted for the N- and C-positions of the free NHO.
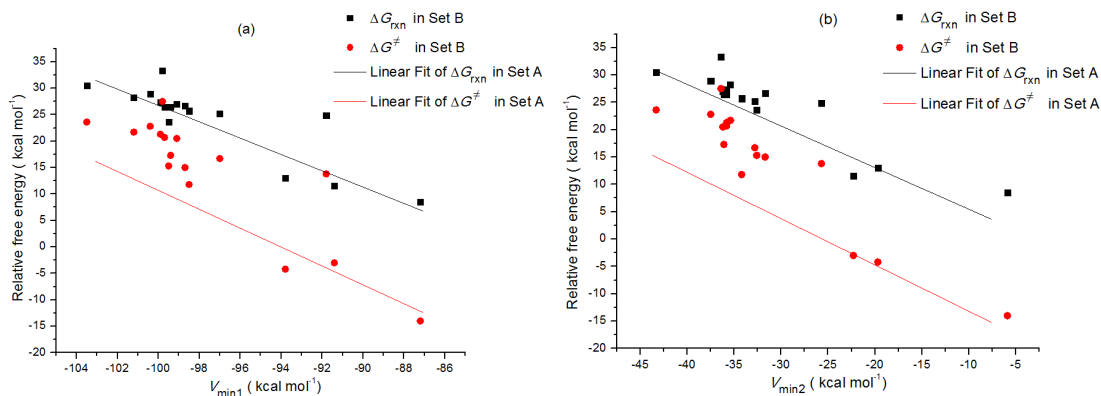
Figure 8 plots the relationship between negatively valued MESP minimums (V_{min1} and V_{min2}) and reaction energies ($\Delta G^{\neq}$ and ΔG_{rxn}) for decarboxylation of NHO–CO$_2$ adducts in set C. These results show that set C is consistent with the general trend that values of $\Delta G^{\neq}$ and ΔG_{rxn} decrease as the negative values for V_{min1} and V_{min2} decrease. Decarboxylation is thermodynamically spontaneous for NHO–CO$_2$ when the electron-withdrawing groups –CO$_2$Me, -CF$_3$, and -CN are at the N- and C-positions. The smaller, negative energy barriers for these adducts mean that decarboxylation is kinetically so favorable that these adducts could not form under the

| R^1 = R^2 = R^3 = Ph | R^1 = R^2 = R^3 = CN | ImBicar | Py[c]BImNMe$_2$ |

V_{min1} = -102.9 V_{min1} = -72.7 V_{min1} = -104.1 V_{min1} = -94.1

V_{min2} = -37.9 V_{min2} = -13.2 V_{min2} = -42.1 V_{min2} = -19.8
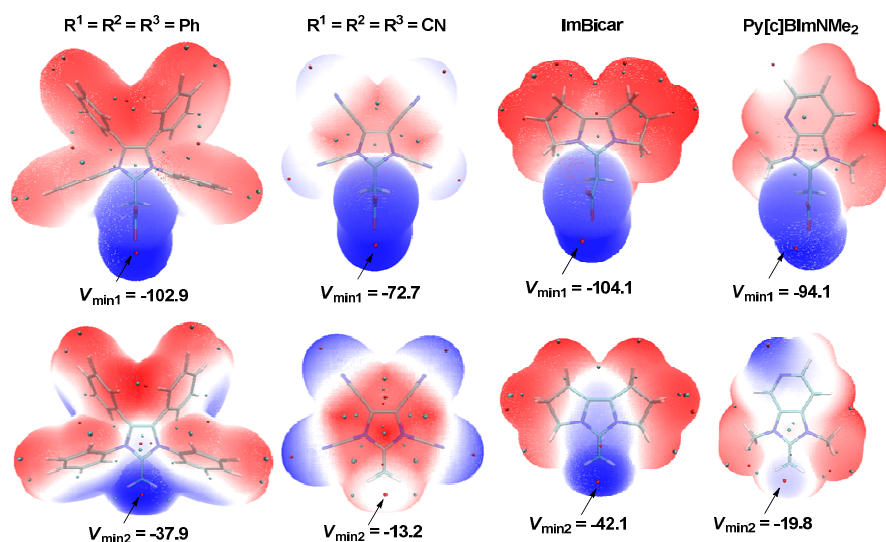
Figure 7 The visualization MESP isosurface of the representative NHO–CO$_2$ adducts and NHOs in Set C and Set D (V_{min1} and V_{min2} values are given in kcal mol^{-1}).

ARTICLE   **Organic & Biomolecular Chemistry**

Table 4 Key bond distance (Å), dihedral angle (º), value of the MESP minimum, the activation free energy, the reaction free energy (all in kcal mol^{-1}), and nucleophilicity indices (eV) of NHO–CO$_2$ adducts and free NHOs in Set C.

R^1 = R^2	R^3 = R^4	d_{C4-C5}	ϑ_1	ϑ_2	$\Delta G^{\neq}$	ΔG_{rxn}	V_{min1}	V_{min2}	N_1	N_2
Me	H	1.558	87.0	0.0	27.0	20.5	−99.1	−36.2	2.2	5.0
Me	Me	1.554	95.3	2.7	28.6	21.8	−101.8	−38.3	2.6	5.2
Me	Me$_2$N	1.556	100.5	3.6	26.7	21.5	−101.6	−37.4	3.0	5.1
Me	Ph	1.557	87.2	0.4	24.2	18.0	−100.3	−33.2	2.6	4.9
Me	MeO	1.558	86.4	5.3	27.2	19.7	−99.8	−33.0	2.8	4.8
Me	F	1.560	85.6	5.1	23.8	15.5	−94.3	−23.4	2.2	4.4
Me	Cl	1.558	96.4	5.4	21.2	15.5	−95.3	−24.5	2.2	4.5
Me	CO$_2$Me	1.560	92.3	9.6	21.8	12.7	−96.6	−26.9	2.0	4.5
Me	CF$_3$	1.560	98.9	4.2	20.7	10.4	−90.7	−19.6	1.8	4.3
Me	CN	1.566	87.0	0.0	17.6	6.7	−85.7	−11.9	1.8	4.2
Me	NO$_2$	1.566	85.9	1.5	17.1	4.6	−84.9	−5.9	1.7	3.9
Me$_2$N	Me$_2$N	1.554	83.5	0.8	27.8	20.9	−106.3	−45.4	2.6	4.7
Ph	Ph	1.561	84.8	0.6	22.5	14.9	−102.9	−37.9	2.5	4.7
MeO	MeO	1.559	88.5	1.7	24.1	6.0	−94.6	−24.8	2.5	3.7
CO$_2$Me	CO$_2$Me	1.569	59.5	16.7	17.0	−6.8	−86.6	−22.3	1.7	3.2
CF$_3$	CF$_3$	1.582	83.3	5.6	9.3	−12.9	−85.0	−7.7	1.5	2.8
CN	CN	1.616	85.0	0.0	−1.8	−25.7	−72.7	13.2	1.4	2.6
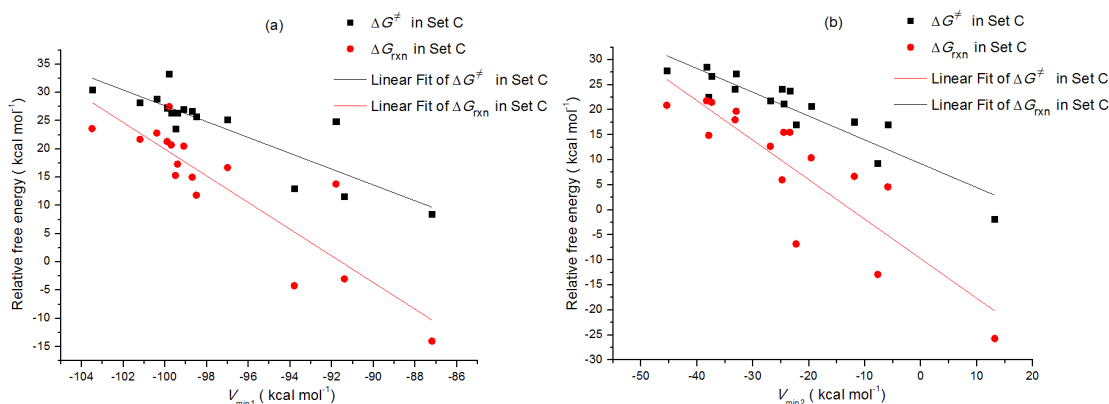
Figure 8. Relationship between the negatively valued MESP minimum (V_{min1} and V_{min2}) and reaction energies ($\Delta G^{\neq}$ and ΔG_{rxn}) for decarboxylation of NHO–CO$_2$ adducts and free NHOs in set C.

the present conditions. The linear correlation between the negatively valued MESP minimums (V_{min1} and V_{min2}) and the free energy barriers ($\Delta G^{\neq}$) in set C is better than seen in set A, owing to the elimination of hydrogen bonding. However, many (V_{min1}, ΔG_{rxn}) and (V_{min2}, ΔG_{rxn}) points deviated from the fitted line, which might have been caused by the steric effect of substituents on the N-positions. For example, decarboxylation of NHO–CO$_2$ adducts containing -NMe$_2$, the most electron-donating group, at the N- and C-positions is thermodynamically more favorable than the one containing the -Me group at the N- and C-positions. Interestingly, both $\Delta G^{\neq}$ (22.5 kcal mol^{-1}) and ΔG_{rxn} (14.9 kcal mol^{-1}) for decarboxylation of NHO−CO$_2$ groups bearing four phenyl groups are much smaller than the ones with phenyl groups substituted on either the N- or C-position. These ΔG values

imply that decarboxylation is thermodynamically and kinetically more favorable.

Based on the calculated nucleophilicity indices, it is found that the combined effect of the electron-withdrawing groups at both N- and C-positions on the reactivity of free NHO is much greater than that from the electron-donating groups. The nucleophilicity index of free NHO containing four -Me groups slightly increases to 5.2 eV, while the nucleophilicity indices of the free NHOs bearing –CO$_2$Me, -CF$_3$ and -CN at the N- and C-positions dramatically fall to 3.2, 2.8, and 2.6 eV, respectively. As a result, these NHO−CO$_2$ adducts might not be effective catalysts for CO$_2$ activation, although they are unstable thermodynamically and kinetically.

Alternatively, saturated or unsaturated rings fused on the N- and C-positions also generate a combined effect on the

stability of NHO–CO$_2$ and free NHO. In set D, the substituents in ImBicar and ImCylm adducts are compared with the NHO–CO$_2$ adduct bearing four -Me groups in set C because both C- and N-positions of these two adducts are connected with saturated hydrocarbon moieties. Notably, the calculated V_{min1} (−104.1 kcal mol^{-1}) and V_{min2} (−42.1 kcal mol^{-1}) of ImBicar are, respectively, 2.3 and 3.8 kcal mol^{-1} more negative than the ones with four -Me groups. These values imply that the electron density at the oxygen anion of the NHO–CO$_2$ adduct and the terminal carbon atom of free NHO is enhanced by introducing additional ring fusion and ring strain next to the imidazolium ring. A similar V_{min1} is observed for the ImCylm adduct, but V_{min2} is slightly lower than that for NHO with four -Me groups. Among all the NHO–CO$_2$ adducts in set C and set D, the nucleophilicity of ImBicar- and ImCylm-free NHOs is comparable with NHOs containing four -Me groups. However, these two adducts are more stable thermodynamically and kinetically. The decomposition of these two adducts must overcome the high free energy barrier of 29.0 kcal mol^{-1}. The overall process is endothermic by 24.0 and 23.0 kcal mol^{-1}, respectively. The V_{min1} and V_{min2} of the ImPhen, BlmNMe$_2$, Py[b]BlmNMe$_2$, and Py[c]BlmNMe$_2$ systems in set D, in which the C- and N-positions are connected with sp^2- and sp^3-hybridized carbon atoms, respectively, can be calculated based on the corresponding set C adduct and NHO with two Me groups substituted on the N-position and two phenyl groups on the C-position. This comparison clearly shows that the V_{min1} and V_{min2} of the four systems in set D are less negative than the corresponding ones in set C, meaning that the placement of unsaturated hydrocarbon moieties on the C-positions will slightly decrease the electron density on the terminal carbon atoms of free NHOs and decrease their nucleophilicity. However, decarboxylation is predicted to be more facile under these conditions. Furthermore, the ImDpylm system can be compared with the NHO–CO$_2$ adducts and NHOs with four phenyl groups substituted on the N-and C-positions set C. V_{min1} and V_{min2} of ImDpylm-free NHO are less negative than those of the reference system, but $\Delta G^{\neq}$ and ΔG_{rxn} for decarboxylation are calculated to be higher by 3.8 and 3.9 kcal mol^{-1}, respectively. These numbers indicate that the ImDpylm adduct might be more stable thermodynamically and kinetically. Meanwhile, the nucleophilicity index of ImDpylm-free NHO is

5.5 eV, meaning that this reactivity might be the highest among all the NHO systems investigated herein.

In summary, the combined effect of C- and N-substituents can more effectively alter the stability of the NHO–CO$_2$ adduct and the reactivity of free NHO. With respect to the NHO–CO$_2$ adduct with 2,6-^{iPr}C$_6$H$_3$ and iPr groups substituted on N-positions for sample **2g**, the NHO–CO$_2$ adduct with four phenyl groups, and the ImPhen and BlmNMe$_2$ adducts show poorer stability thermodynamically and kinetically, as indicated by a smaller $\Delta G^{\neq}$ (22.5, 22.6 and 21.2 kcal mol^{-1}) and ΔG_{rxn} (14.9, 14.7, and 12.6 kcal mol^{-1}) for decarboxylation. The nucleophilicity indices of these free NHOs are slightly lower (4.6 and 4.7 eV). In terms of the balance between the stability of NHO–CO$_2$ adducts and the nucleophilicity of the corresponding free NHOs, these three NHO–CO$_2$ adducts are predicted to exhibit higher catalytic activity in the carboxylative cyclization of propargylic alcohols with CO$_2$.[9]

Conclusions

In the present work, the effect of substituents on the stability of NHO–CO$_2$ adducts and the reactivity of free NHOs was theoretically investigated by the combination of DFT calculations, MESP, and global nucleophilicity indices analysis. The major conclusions are listed below:

1. The nucleophilicity indices analysis confirms that free NHOs are stronger nucleophiles than NHO–CO$_2$ adducts. Hence, the thermodynamically and kinetically unstable NHO–CO$_2$ adducts should be more efficient organocatalysts for nucleophile-promoted reactions.

2. The stability of NHO–CO$_2$ adducts as well as the reactivity of free NHOs are significantly influenced by the C- and N-substituents. The C-substituent exerts an electronic effect only. The electron-withdrawing C-substituent decreases the electron density on the carboxyl moiety of NHO–CO$_2$ and the terminal carbon atom of olefins, which favors decarboxylation but weakens the nucleophilicity of NHO. The N-substituent contributes both electronic and steric effects. As the steric bulk of the N-alkyl group increases, the stability of the NHO–CO$_2$ adducts and reactivity of free NHO slightly increase.

3. The balance between the stability of NHO–CO$_2$ adducts

Table 5 Key bond distance (Å), dihedral angle (º), value of the MESP minimum, the activation free energy, the reaction free energy (all in kcal mol^{-1}), and the nucleophilicity indices (eV) of NHO−CO$_2$ adducts and free NHOs in Set D.

System	d_{C4-C5}	ϑ_1	ϑ_2	$\Delta G^{\neq}$	ΔG_{rxn}	V_{min1}	V_{min2}	N_1	N_2
ImBicar	1.553	80.1	0.6	29.0	24.0	−104.1	−42.1	2.6	5.2
ImCylm	1.554	84.6	2.4	29.0	23.0	−103.0	−37.7	2.8	5.1
ImDpylm	1.558	76.2	5.9	26.3	18.9	−102.2	−30.8	3.5	5.5
ImPhen	1.558	87.8	0.1	22.6	14.7	−99.2	−30.5	2.6	4.7
BlmNMe$_2$	1.559	88.5	0.0	21.2	12.6	−98.1	−26.8	2.3	4.6
Py[b]BlmNMe$_2$	1.563	89.7	1.4	17.6	7.3	−96.1	−22.6	2.1	4.3
Py[c]BlmNMe$_2$	1.562	78.3	4.3	17.8	7.1	−94.1	−19.8	2.0	4.2

and the reactivity of free NHOs can be tuned by the combined effect of C- and N-substituents. NHO–CO_2 adducts with a weak electron-withdrawing group (unsaturated hydrocarbon moieties or -Ph) at the C-position, and a bulk aromatic substituent or ring strain at the N-position, is predicted to result in a more efficient catalyst for the carboxylative cyclization of propargylic alcohols with CO_2.

Further studies to understand the reaction mechanism of carboxylative cyclization catalyzed by NHO–CO_2 adducts as well as the catalytic performance of NHO–CO_2 adducts presented in this paper is ongoing in our group.

Acknowledgements

Notes and References

1   For reviews see: (a) G. Fiorani, W. Guo, and A. W. Kleji, *Green Chem.*, 2015, **17**, 1375; (b) I. Omae, Coord. *Chem. Rev.*, 2012, **256**, 1384; (c) S. N. Riduan and Y. Zhang, *Dalton Trans.*, 2010, **39**, 3347; (d) D. J. Darensbourg, *Inorg. Chem.* 2010, **49**, 10765.

2   (a) L. Yang, and H. Wang, ChemSusChem, 2014, 962; (b) Z. Z. Yang, L. N. He, J. Gao, A. H. Liu, and B. Yu, *Energy Environ. Sci.*, 2012, **5**, 6602; (c) M. B. Ansari, and S. e. Park, *Energy Environ. Sci*., 2012, **5**, 9419.

3   (a) M. Aresta, and C. F. Nobile, *J. Chem. Soc. Chem. Commun.*, 1975, 636; (b) M. Aresta, and Nobile, C. F. *J. Chem. Soc. Dalton. Trans.,* 1977, 709; (c) S. Gambarotta, F. Arena, C. Floriani, and P. F. Zanazzi, *J. Am. Chem. Soc.,* 1982, **104**, 5082; (d) J. C. Calabrese, T. Herskovitz, and J. B. Kinney, *J. Am. Chem. Soc.,* 1983, **105**, 5914.

4   (a) D. Enders, O. Niemeier and A. Henseler, *Chem. Rev.*, 2007, **107**, 5606; (b) N. Marion, S. DiezGonzalez and S. P. Nolan, *Angew. Chem., Int. Ed.,* 2007, **46**, 2988; (c) C. Ma and Y. Yang, *Org. Lett.,* 2005, **7**, 1343; (c) C. Ma, H. Ding, Y. Zhang and M. Bian, *Angew. Chem., Int. Ed.*, 2006, **45**, 7793; (e) D. Enders, O. Niemeier and A. Henseler, *Chem. Rev.*, 2007, **107**, 5606. (f) J. L. Moore and T. Rovis, *Top. Curr. Chem.*, 2010, **291**, 77.

5   (a) H. Zhou, W. Zhang, C. Liu, J. Qu and X. Lu, *J. Org. Chem.*, 2008, **73**, 8039. (b) B. R. Van Ausdall, J. L. Glass, K. M. Wiggins, A. M. Arif and J. Louie, *J. Org. Chem.*, 2009, **74**, 7935; (c) M. J. Ajitha and C. H. Suresh, *J. Org. Chem.*, 2012, **77**, 1087.

6   (a) S. N. Riduan, Y. Zhang and J. Y. Ying, *Angew. Chem., Int. Ed.*, 2009, **48**, 3322; (b) V. Nair, V. Varghese, R. R. Paul, A. Jose, C. R. Sinu and R. S. Menon, *Org. Lett.*, 2010, **12**, 2653；(c) Y. Kayaki, M. Yamanoto, and T. Ikariya, *Angew. Chem., Int. Ed.*, 2009, **48**, 4194; (d) A. Ueno, Y. Kayaki and T. Ikariya, *Green Chem.*, 2013, **15**, 425.

7   (a) F. Huang, G. Lu, L. Zhao, H. Li and Z. Wang, *J. Am. Chem. Soc.*, 2010, **132**, 12388; (b) X. Ren, Y. Yuan, Y. Ju and H. Wang, *ChemCatChem*, 2012, **4**, 1943; (c) M. J. Ajitha and C. H.

Suresh, *Tetrahedron Lett.*, 2011, **52**, 5403; W. Li, D. Huang, Y. Lv, Rsc. Adv., 2014, **4**, 17236.

8   (a) W. Kantlehner, In *Science of Synthesis*, A. de Meijere, Ed., *Thieme: Stuttgart*, 2006, 24, 571; (b) P. A. Keller, J. Morgan, In *Science of Synthesis*, A. de Meijere, Ed., *Thieme: Stuttgart*, 2006. 24, 707; (c) A. Fürstner, M. Alcarazo, R. Goddard, and C. W. Lehmann, *Angew. Chem., Int. Ed.*, 2008, **47**, 3210; (d) A. Glöckner, S. Kronig, T. Bannenberg, C. G. Daniliuc, P. G. Jones, and M. Tamm, *J. Organomet. Chem.*, 2013, **723**, 181; (e) S. M. I. Al-Rafia, A. C. Malcolm, S. K. Liew, M. J. Ferguson, McDonald, and E. Rivard, *Chem. Commun.,* 2011, **47**, 6987; (f) B. Maji, M. Horn, and H.Mayr, *Angew. Chem., Int. Ed.,* 2012, **51**, 6231; (g) S. Kronig, P, G. Jones, M. Tamm, *Eur. J. Inorg. Chem.,* 2013, 2301.

9   Y. B. Wang, Y. M. Wang, W. Z. Zhang, and X. B. Lu, *J. Am. Chem. Soc.*, 2013, **135**, 11996.

10 M. J. Frisch, et al. *Gaussian 09, Reversion A.02*; Gaussian, Inc., Wallingford CT, 2009.

11 (a) Y. Zhao and D. G. Truhlar, *Theor. Chem. Acc.*, 2008, **120**, 215; (b) Y. Zhao and D. G. Truhlar, *Acc. Chem. Res.*, 2008, **41**, 157.

12 A. V. Marenich, C. J. Cramer, and D. G. Truhlar, *J. Phys. Chem. B* 2009, **113**, 6378.

13 (a) R. Ditchfield, W. J. Hehre and J. A. Pople, *J. Chem. Phys.*, 1971, **54**, 724; (b) W. J. Hehre, R. Ditchfield and J. A. Pople, *J. Chem. Phys.,* 1972, **56**, 2257; (c) P. C. Hariharan and J. A. Pople, *Mol. Phys.,* 1974, **27**, 209; (d) M. S. Gordon, *Chem. Phys. Lett.,* 1980, **76**, 163; (e) P. C. Hariharan and J. A. Pople, *Theor. Chem. Acc.,* 1973, **28**, 213; (f) J. P. Blaudeau, M. P. McGrath, L. A. Curtiss and L. Radom, *J. Chem. Phys.*, 1997, **107**, 5016; (g) M. M. Francl, W. J. Pietro, W. J. Hehre, J. S. Binkley, M. S. Gordon, D. J. DeFrees and J. A. Pople, *J. Chem. Phys.*, 1982, **77**, 3654; (h) R. C. Binning, Jr and L. A. Curtiss, *J. Comput. Chem.*, 1990, **11**, 1206; (i) V. A. Rassolov, J. A. Pople, M. A. Ratner and T. L. Windus, *J. Chem. Phys.,* 1998, **109**, 1223; (j) V. A. Rassolov, M. A. Ratner, J. A. Pople, P. C. Redfern and L. A. Curtiss, *J. Comput. Chem.*, 2001, **22**, 976.

14 (a) M. Gutowski, G. Chalasinski, *J. Chem. Phys.,* 1993, **98**, 5540; (b) K. Szalewicz, B. Jezioski, *J. Chem. Phys.,* 1996, **109**, 1198; (b) G. Lendvay, I. Mayer, *Chem. Phys. Lett.*, 1998, **297**, 365; (c) N. Kobko, J. J. Dannenber, *J. Phys. Chem. A* 2001, **105**, 1944.

15 (a) C. P. Kelly, C. J. Cramer, D. G. Truhlar, *J. Chem. Theory. Comput.* 2005, **1**, 1133; (b) C. P. Kelly, C. J. Cramer, D. G. Truhlar, *J. Phys. Chem. B* 2006, **1**, 16066. (c) V. S. Bryantsev, M. S. Diallo, W. A. Goddard III, J. Phys. Chem. *B* 2008, **112**, 9709.

16 (a) P. Politzer, and D. G. Truhlar, *Chemical applications of atomic and molecular electrostatic potentials: reactivity, structure, scattering, and energetics of organic, inorganic, and biological systems*; Plenum Press: New York, 1981. (b) S. R. Gadre, R. N. and Shirsat, *Electrostatics of Atoms and Molecules*; Universities Press: Hyderabad, India, 2000.

17 (a) B. Galabov, S. Ilieva, and H. F. Schaefer, III *J. Org. Chem.*, 2006, **71**, 6382; (b) P. Politzer, and J. S. Murray, *Theor. Chem. Acc.*, 2002, **108**, 134; (c) S. R. Gadre, and C. H. Suresh, *J. Org. Chem.*, 1997, **62**, 2625; (d) C. H. Suresh,and S. R. Gadre, *J. Am. Chem. Soc.*, 1998, **120**, 7049; (e) C. H. Suresh, *Inorg. Chem.*, 2006, **45**, 4982; (f) C. H. Suresh, and S. R. Gadre, *J. Phys. Chem. A* 2007, **111**, 710; (g) J. Mathew, T. Thomas, and C. H. Suresh, *Inorg. Chem.*, 2007, **46**, 10800; (h) F. B. Sayyed, and C. H. Suresh, *New J. Chem.*, 2009, **33**, 2465; (i) F. B. Sayyed, C. H. Suresh,and S. R. Gadre, *J. Phys. Chem. A* 2010, **114**, 12330; (j) M. M. Deshmukh, S. R. Gadre, R. Tonner, and G. Frenking, *Phys. Chem. Chem. Phys.,* 2008, 10, 2298; (k) K. C. Gross, P. G. Seybold, Z. Peralta-Inga, J. S. Murray, and P. Politzer, *J. Org. Chem.*, 2001, **66**, 6919; (l) R. V. Pinjari, S. P. Gejji, *J. Phys. Chem. A* 2008, **112**, 12679.

12 | *Org*. *Biomol. Chem*., 2015, **00**, 1-3

This journal is © The Royal Society of Chemistry 20xx

ARTICLE

18 (a) T. Lu, and F. Chen, *J. Comp. Chem*., 2012, **33**, 580; (b) T. Lu, and F. Chen, *J. Mol. Graph. Model.*, 2012, **38**, 314.

19 (a) L. R. Domingo and J. A. Sáez, *Org. Biomol. Chem.*, 2009, **7**, 3576; (b) L. R. Domingo, E. Chamorro and P. Pérez, *J. Org. Chem*., 2008, **73**, 4615; (c) R. G. Parr, L. von Szentpály and S. Liu, *J. Am. Chem. Soc*. 1999, **121**, 1922.

20 The nucleophilicity is taken relative to tetracyanoethylene (TCE) as a reference, because it has the lowest HOMO energy in a large series of molecules already investigated in the context of polar cycloadditions.

21 C. Y. Legault, CYLview, 1.0b, Université de Sherbrooke: Sherbrooke, Québec, Canada, 2009 (http://www.cylview.org).

22 W. Humphrey, A. Dalke, and K. Schulten, *J. Mol. Graph. Model.*, 1996, **14**, 33.

23 P. Jaramilio, L. R. Domingo, E. Chamorro, P. Pérez, *J. Mol. Stru.: THEOCHEM*, 2008, **865**, 68.

Organic & Biomolecular Chemistry Accepted Manuscript